Nanorod Assembly

DOI: 10.1002/anie.200904118

Gemini-Surfactant-Directed Self-Assembly of Monodisperse Gold Nanorods into Standing Superlattices**

Andrés Guerrero-Martínez, Jorge Pérez-Juste, Enrique Carbó-Argibay, Gloria Tardajos, and Luis M. Liz-Marzán**

Fabrication of ordered nanoparticle assemblies over extended areas and volumes is still a major challenge in nanomaterials research.[1] The current limitations in the production of such ordered assemblies dramatically hinder the application of nanoparticles in fields such as negative refractive index metamaterials or information technologies. In the particular case of metal nanocrystal assemblies,[2] nanoscale organization of readily accessible spherical gold nanoparticles[3,4] has been manipulated to produce a diverse range of topologies[5] with interesting optical and electrical properties.[6,7] However, the use of isotropic nanoparticles strongly limits potential applications that require the formation of lattices with vectorial properties. A recent report[8] demonstrated the formation of 3D gold nanorod (NR) superstructures from liquid-crystalline phases[9–12] with a limited degree of control over the dimensionality and directionality of the assembly. A major advance is demonstrated herein through the use of a gemini surfactant.[13] Replacement of cetyltrimethylammonium bromide (CTAB) by this unconventional surfactant during nanorod synthesis leads to production of monodisperse NRs that can undergo directional self-assembly into highly ordered 2D and 3D standing superlattices with anisotropic optical properties.

The synthesis of highly monodisperse gold NRs is especially appealing because of their strong, polarization-dependent suface-plasmon-based optical properties,[14] which render their assemblies ideal candidates for the preparation of optically anisotropic lattices that allow manipulation of light in the nanoscale.[15] Nowadays, tuning of the longitudinal and transverse localized plasmon resonances of gold NRs by synthetic manipulation is a mature field of research. In particular, the seeded growth method in aqueous solution,[16] based on the reduction by a weak reducing agent of a gold salt on premade small seeds in the presence of CTAB and silver ions provides sufficient flexibility to synthesize nanorods (CTAB-NRs) with diverse sizes and shapes.[17] Besides being a shape-inducing agent, CTAB efficiently prevents aggregation through dynamic adsorption onto the gold NRs surface in a bilayer fashion.[18] This nanoparticle shielding of CTAB in water, together with the intense capillary forces generated at the solvent–air interfaces in aqueous solution and the typical Brownian motion of nanoparticles, brings colloidal stability face-to-face with controlled self-assembly of NRs in water and demands a rational search for new and simple strategies.

To date, the construction of assemblies of standing gold NRs has mostly relied on postsynthesis surface functionalization with thiol and silane capping agents[19,20] and subsequent transfer into organic solvents. However, the degree of order in the self-assembly has still been limited to 2D sub-micrometer areas. Among the different capping agents that have been proposed for the preparation of metal nanoparticle arrays in organic solvents, thiol-functionalized phospholipid derivatives have proven excellent binders in nanoparticle–lipid–nanoparticle assemblies,[19,21] as they can be efficiently supported as bilayers on different substrates. In this respect, gemini surfactants, made of two hydrophobic tails and two hydrophilic headgroups linked by a spacer chain, are currently available as excellent scaffolds for structurally mimicking the bilayer formation of lipids in water.[22] Moreover, gemini surfactants display exceptional amphiphilic properties,[23] such as high adsorptivities on solid surfaces, which make them ideal candidates to influence the growth[24,25] and assembly of gold nanorods. We present herein the first study in which cationic gemini surfactants, (oligooxa)alkanediyl-α,ω-bis(dimethyldodecylammonium bromide) (12-EO$_x$-12, see the Supporting Information), were used for the reproducible and controlled synthesis of monodisperse gold NRs, focusing on the role of the chemical structure of these surfactants on the self-assembly of highly ordered, robust 2D and 3D gold NR superlattices with directional optical properties.

We synthesized gold nanorods using the gemini surfactant that contains a spacer with one ethylene oxide group, 12-EO$_1$-12 (Gem1-NRs), as a shape-directing agent by Ag^+-assisted seeded growth[26] on preformed CTAB-capped gold seeds at 27 °C (see details in the Experimental Section). Controlling the molar ratio between seed and gold salt, the aspect ratio and longitudinal surface plasmon (LSP) resonance of the NRs could be readily tuned (see the Experimental Section). Significantly narrower LSP bands were measured for Gem1-NRs than for CTAB-NRs, with typical full width at half LSP maximum (FWHM) reduction of 20–30 % (see the Support-

[*] Dr. A. Guerrero-Martínez, Dr. J. Pérez-Juste, E. Carbó-Argibay, Prof. L. M. Liz-Marzán
Departamento de Quimica Fisica and Unidad Asociada CSIC
Universidade de Vigo, 36310 Vigo (Spain)
Fax: (+34) 986-812556
E-mail: aguerrero@uvigo.es
lmarzan@uvigo.es
Prof. G. Tardajos
Departamento de Química-Física I, Facultad de Ciencias Químicas
Universidad Complutense de Madrid, 28040 Madrid (Spain)

[**] A.G.-M. acknowledges the Juan de la Cierva Program (MICInn, Spain). This work has been funded by the Spanish Ministerio de Ciencia e Innovación (MAT2007-62696) and by the EU (NANO-DIRECT, grant number CP-FP 213948-2).

Supporting information for this article is available on the WWW under http://dx.doi.org/10.1002/anie.200904118.

ing Information). These results are in good agreement with an improved monodispersity observed in transmission electron microscopy (TEM) images (see the Supporting Information), and they highlight the advantage of using this gemini surfactant to prepare monodisperse gold NRs with improved standard deviations (see the Experimental Section). We attribute this monodispersity to a highly restrained growth of gold NRs in the presence of gemini surfactant micelles, arising from structural rigidity at the surfactant–nanoparticle interface.

While the precise mechanism involved in the anisotropic growth of gold CTAB-NRs in the seeded growth method is not completely understood at a molecular level, silver underpotential deposition (UPD) and adsorption of CTAB on NRs have been proposed as key factors.[26,27] In this surfactant contribution, known as a "zipping" mechanism, the van der Waals interactions between hydrophobic tails within the CTAB bilayer would favor the longitudinal growth of the nanorod. On the basis of this model, the differences between Gem1-NRs and CTAB-NRs can arise from two factors: 1) differences in the morphologies of CTAB and gemini micelles; 2) different packing at the interface with hydrophilic surfaces. Whereas CTAB forms spherical micelles in aqueous solution under the experimental conditions of synthesis, gemini surfactants with short chain spacers, such as 12-EO_1-12, can build up worm-like micelles.[28] The ethylene oxide spacer leads to micelle elongation owing to an increased distance between headgroups as compared to CTAB, and it results in a lower curvature of micelles at the surfactant–water interface. Incidentally, aggregates at hydrophilic surfaces follow the same curvature trend, ranging from parallel cylinders to bilayers for CTAB and gemini surfactants, respectively.[29] All of these differences suggest a closer packing of 12-EO_1-12 at the bilayer–nanoparticle interface as compared to CTAB, resulting in an increased rigidity that may affect the dynamic mechanism behind NR growth. Additionally, the less flexible conformation of the bilayer might induce stronger adsorption of silver onto the NR surface (through UPD[26]), thereby improving monodispersity in Gem1-NRs.

A direct consequence of NR monodispersity and the interfacial aggregation properties of 12-EO_1-12 at solid–liquid interfaces can be observed in the TEM images (Figure 1) in the form of spontaneous formation of self-assembled monolayers of standing Gem1-NRs by simple drop casting on carbon-coated TEM grids. Detailed analysis of the assembly revealed that the concentration of gold Gem1-NRs (for constant 12-EO_1-12 surfactant concentration of 10^{-3} M, slightly above its critical micelle concentration (CMC)[30]), significantly affected the extension of the self-assembled areas. Whereas side-by-side assemblies of a few NRs were observed at low particle concentrations (10^{-10} M, Figure 1a), well-defined islands with a significantly larger monolayer extension were observed at higher concentration (10^{-8} M). Figure 1b shows islands with micrometer areas covered by approximately 10000 standing Gem1-NRs. At analogous experimental conditions, no ordered self-assembly was observed with CTAB-NRs (Figure 1c). A closer view of one of these islands revealed the striking long-range order of the

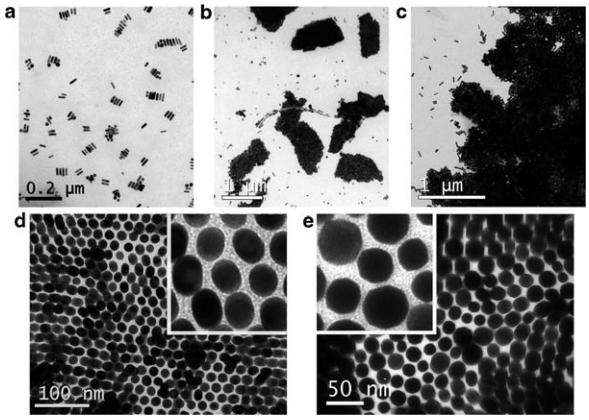

Figure 1. Representative TEM micrographs of gold NRs with 12-EO_1-12 or CTAB. a) Examples of side-by-side assembled Gem1-NRs obtained at low nanoparticle concentration (10^{-10} M). b) Gem1-NR islands formed by standing NR monolayers produced by drop-casting onto TEM grids (10^{-8} M). c) Typical disordered CTAB-NR aggregates under the same experimental conditions as (b). d) Representative image of the hexagonally packed monolayer of monodisperse Gem1-NRs. e) Monolayer of NRs synthesized with CTAB, which was then replaced with 12-EO_1-12. Gold NRs are oriented along the growth direction [001], showing the facetted crystal structure of the rods with octagonal cross section.

assembly with a hexagonal close-packed arrangement of Gem1-NRs within the monolayer (Figure 1d). The importance of the gemini surfactant in the formation of ordered monolayers was confirmed upon exchange of CTAB from CTAB-NRs with 12-EO_1-12 (the interfacial self-assembly of gemini surfactants with short spacers onto the gold NR surface is dominated by stronger headgroup–surface electrostatic interactions than those in CTAB).[29] As shown in Figure 1e, upon incorporation of 12-EO_1-12 on the NR surfaces, standing monolayers were obtained, just like for Gem1-NRs. These monolayers displayed a shorter-range order, owing to the lower monodispersity of CTAB-NRs, which creates defects in the 2D crystalline structure (see insets of Figure 1d,e). Therefore, higher monodispersity and surface properties of Gem1-NRs are ideal to study the self-assembly of gold NRs as building blocks of 2D and 3D superlattices.

When a more concentrated Gem1-NR colloid (10^{-6} M) was drop cast on a silicon wafer, the resulting deposition of gold NRs typically resulted in formation of rings (coffee-cup effect) 40–60 μm wide with 1–2 mm external diameter and a significant amount of cracks (Figure 2a). As clearly shown in Figure 2b, Gem1-NRs self-assemble into islands that span 1–10 μm across, with an extraordinary long-range order. Figure 2c shows a representative scanning electron microscopy (SEM) image of a highly ordered, multilayer 3D array with hexagonal arrangement. The fast Fourier transform of the image confirms perfect hexagonal geometry, with an average distance between the centers of neighboring metal particles of (14.9 ± 0.9) nm. The striking long-range ordered multilayer structure of this particular Gem1-NRs array can be gathered from Figure 2d, in which a lateral view of an island shows up to 14 layers of free-standing NRs. As expected from the hexagonal arrangement, each NR monolayer is shifted by half

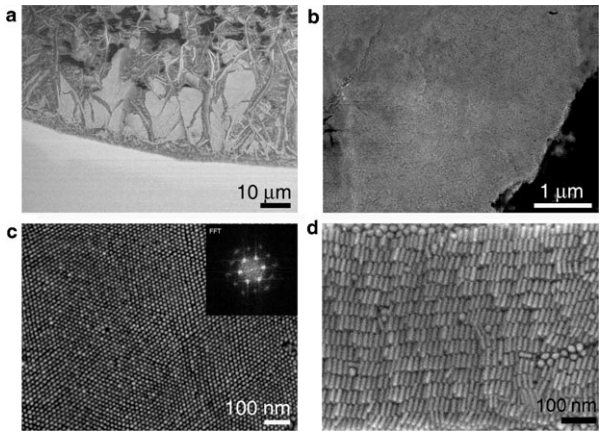

Figure 2. SEM micrographs of gold Gem1-NRs on a silicon wafer obtained at high concentration (10^{-6} M). a) Partial view of the ring formed upon casting. b,c) Top view of the ordered nanocrystal superlattice at different magnifications. The inset in (c) is the fast Fourier transform of the image. d) Side view of an island in which 14 layers of standing NRs can be distinguished.

the inter-NR distance with respect to the adjacent layers. While several recent reports have been published on the preparation of 2D standing arrays of gold nanorods,[19,20] the quality and extension of these 2D and 3D standing superlattices is unprecedented.

Analogous oriented superlattices of gold NRs were obtained on ITO-covered glass substrates (see the Supporting Information; ITO = indium tin oxide), which present high transparency and conductivity and are thus of interest for potential optoelectronic applications. As the longitudinal and transverse localized surface plasmon resonances of gold nanorods are basically independent of each other, the collective transverse plasmon mode of the standing Gem1-NRs within a superlattice can be selectively excited by using non-polarized Vis/NIR irradiation. This effect is illustrated in Figure 3a, which shows an optical photograph of the edge of a

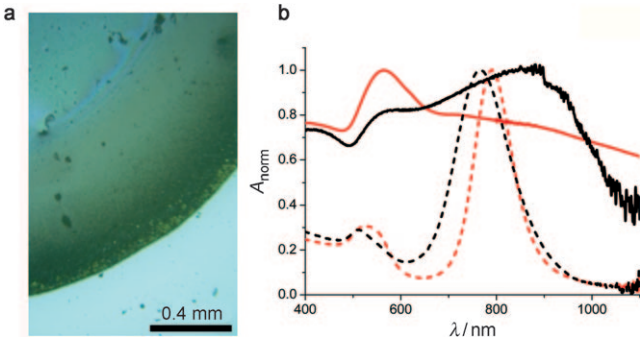

Figure 3. a) Photograph of a partial view of the ring formed upon drop casting of a NR colloid, which was acquired in reflection mode under white-light illumination. b) UV/Vis/NIR spectra of Gem1-NR (red) and CTAB-NR (black) isotropic solutions in water (dashed lines) and their corresponding assemblies onto ITO-coated glass (solid lines). The Gem1-NR array profile reflects the high order of standing NRs and the anisotropic nature of the surface. Note that Gem1-NRs show a significantly narrower LSP band than CTAB-NRs in aqueous isotropic solutions.

NR ring assembly formed on an ITO-coated glass substrate, from which the Vis/NIR spectrum of the Gem1-NRs array was measured. Figure 3b shows the spectrum of the assembly together with that of the isotropic Gem1-NRs aqueous solution. Whereas the spectrum in solution displays two well-defined bands corresponding to the transverse and longitudinal plasmon modes, only the transverse plasmon band is excited in the array, which is macroscopic evidence of the nearly perfect perpendicular alignment of the NRs within the superlattice. As expected, broadening and red shift of the transverse plasmon band occurred, as a consequence of plasmon coupling between the close-packed NRs.[31] In contrast, no selective excitation of the transverse plasmon band was observed when CTAB-NRs were assembled in a similar fashion, but instead a broad and red-shifted band revealed a random distribution of aggregated NRs on the substrate.

The binding effects of 12-EO_1-12 resulting from the formation of thousands of van der Waals and electrostatic bonds at the NR–bilayer–NR interfaces combine to lend overall stability to the 2D and 3D arrays. The fact that small side-by-side aggregates are formed at low particle concentration suggests that the 3D assemblies obtained from more highly concentrated solutions develop during the evaporation process by merging of bilayers formed in solution (Figure 4a).

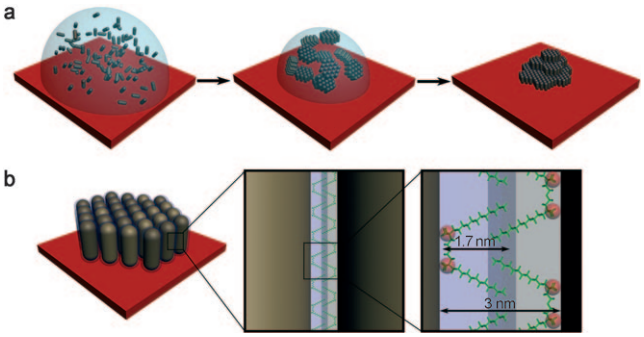

Figure 4. a) Schematic diagram of different stages during drying, showing the initial random distribution of Au NRs in the isotropic solution, self-assembly during drying, formation of smectic-B liquid-crystalline phases, and final generation of 3D superlattices of standing NRs. b) Representation of a Gem1-NR monolayer, in which bilayers of 12-EO_1-12 bind two adjacent NRs by strong van der Waals hydrophobic interactions of the alkyl chains (blue region), and intense electrostatic interactions at the NR surface owing to both gemini binding sites (red spheres).

These 3D superstructures can result from the formation of smectic-B liquid-crystalline phases[8–10] in which all the Gem1-NRs are oriented in layers with the same orientation and with a hexagonal arrangement, leading to micrometer-sized self-assembled areas upon solvent evaporation. Assuming a surfactant bilayer structure of gold NRs around 12 nm thick, and considering a separation of approximately 15 nm between the centers of two NRs in the array (Figure 2c), a minimum distance between gold NR surfaces can be estimated at approximately 3 nm, a value that is in agreement with TEM. Taking into account geometrical considerations

for 12-EO_1-12, in which the length of one of the cationic alkyl chains is around 1.7 nm when completely extended, we propose a simple model of surfactant–nanoparticle interaction in which a gemini surfactant bilayer is connected to two NRs (Figure 4b), in agreement with the tendency of gemini surfactants with short head-to-head distances to build up bilayers on hydrophilic surfaces.[29] This model considers at a molecular level two areas of interaction that will be responsible for the long-range self-assembly (Figure 4b): 1) a region of intense van der Waals hydrophobic interactions arising from the interpenetration of the gemini surfactant alkyl chains, and 2) intense electrostatic interactions at the NR surface level because of the presence of two (charged) surfactant binding sites.

Finally, to confirm the proposed interaction model, we synthesized gold NRs in the presence of a gemini surfactant with a longer spacer, 12-EO_4-12 (Gem4-NRs). We found that Gem4-NRs present dimensions and aspect ratio standard deviations that are similar to those for CTAB-NRs. Moreover, no ordered assemblies were obtained by drop-casting on solid substrates. These results are consistent with the proposed model for the self-assembly of Gem1-NRs. While cationic gemini surfactants with short ethylene oxide spacers form bilayers at the interface with hydrophilic substrates, gemini surfactants with longer spacers, such as 12-EO_4-12, exhibit rod-like aggregates, analogously to CTAB micelles.[28] This bilayer-to-cylindrical transition as a function of surfactant geometry has been associated with the high flexibility and folding of long ethylene oxide chains in aqueous solution.[32] Thus, shorter distances between polar head groups of 12-EO_4-12 inside aggregates result in higher curvatures and flexibilities of the interfacial film, thus decreasing the interaction area with the gold substrate and hindering the self-assembly of NRs.

Future prospects envisage the use of gemini surfactants, with different alkyl chains and spacers, or with additional binding sites, in the highly controlled synthesis and self-assembly of different anisotropic metal nanoparticles. Further analysis and optimization of self-assembly conditions may allow the design of large-scale, geometrically controlled functional materials with macroscopic-scale spatially dependent properties. Additionally, this system of monodisperse nanorods readily forming colloidal crystals can open new avenues toward understanding and quantitative characterization of colloidal phase behavior of short nanorods.

Experimental Section

Gemini surfactants, 12-EO_1-12 and 12-EO_4-12 were synthesized according to procedures described in the literature.[30,32] Gold nanorods were prepared by seeded growth[16,18] at 27 °C through reduction of $HAuCl_4$ with ascorbic acid on CTAB-stabilized Au nanoparticle seeds (smaller than 3 nm) in the presence of CTAB (0.1 M) or 12-EO_x-12 (0.05 M), HCl (pH 2–3), and $AgNO_3$ (0.12 mM). After synthesis, the gold nanorod solution (5 mL) was centrifuged twice (8000 rpm, 20 min) to remove excess reactants. One thousand particles were measured on TEM images of each sample to determine the average length and width of the rods. Gem1-NRs and CTAB-NRs samples with different aspect ratios were prepared for the size dispersion analysis (average aspect ratio, length, thickness, LSP maximum, FWHM) of Gem1-NRs (3.1 ± 0.4, 34 ± 7 nm, 10 ± 2 nm, 748 nm, 50 nm / 4.1 ± 0.6, 42 ± 7 nm, 10 ± 2 nm, 820 nm, 63 nm) and CTAB-NRs (3.1 ± 0.6, 41 ± 10 nm, 13 ± 3 nm, 748 nm, 71 nm / 3.9 ± 0.8, 35 ± 9 nm, 9 ± 2 nm, 827 nm, 80 nm). The errors of aspect ratio and dimensions represent standard deviations.

2D and 3D arrays were formed on carbon grids, silicon wafers, and ITO-coated glass slides using solutions of monodisperse Gem1-NRs in water, with average aspect ratio, length, and width of 3.6 ± 0.4, (43 ± 8) nm, and (12 ± 2) nm, respectively. CTAB-NRs and Gem4-NRs with similar dimensions were used for comparison. To control the extent of the self-assembly, the concentration of surfactants (1.2 mM) was maintained above the respective CMC, and different concentrations of particles were used, ranging from 10^{-9} to 10^{-6} M. Droplets (10 μL) were evaporated under ambient conditions, and the final drying stage took place after several hours.

Optical characterization was carried out by UV/Vis/NIR spectroscopy with a Cary 5000 spectrophotometer using 10 mm path length quartz cuvettes for aqueous NRs solutions and 1 mm thick ITO slides for NR assemblies. TEM images were obtained with a JEOL JEM 1010 transmission electron microscope operating at an acceleration voltage of 100 kV. SEM images were obtained using a JEOL JSM-6700F FEG microscope operating at 3.0 kV for secondary-electron imaging (SEI).

Received: July 24, 2009
Published online: October 2, 2009

Keywords: anisotropy · gold · nanostructures · self-assembly · surfactants

[1] E. V. Shevchenko, D. V. Talapin, N. A. Kotov, S. O'Brien, C. B. Murray, *Nature* **2006**, *439*, 55.
[2] S. Narayanan, J. Wang, X.-M. Lin, *Phys. Rev. Lett.* **2004**, *93*, 135503.
[3] B. A. Korgel, D. Fitzmaurice, *Phys. Rev. Lett.* **1998**, *80*, 3531.
[4] T. P. Bigioni, X.-M. Lin, T. T. Nguyen, E. I. Corwin, T. A. Witten, H. M. Jaeger, *Nat. Mater.* **2006**, *5*, 265.
[5] M.-C. Daniel, D. Astruc, *Chem. Rev.* **2004**, *104*, 293.
[6] M. D. Musick, C. D. Keating, L. A. Lyon, S. L. Botsko, D. J. Peña, W. D. Holliway, T. M. McEvoy, J. N. Richardson, M. J. Natan, *Chem. Mater.* **2000**, *12*, 2869.
[7] S. W. Boettcher, N. C. Strandwitz, M. Schierhorn, N. Lock, M. C. Lonergan, G. D. Stucky, *Nat. Mater.* **2007**, *6*, 592.
[8] T. Ming, X. Kou, H. Chen, T. Wang, H.-L. Tam, K.-W. Cheah, J.-Y. Chen. , J. Wang, *Angew. Chem.* **2008**, *120*, 9831; *Angew. Chem. Int. Ed.* **2008**, *47*, 9685.
[9] F. M. van der Kooij, K. Kassapidou, H. N. W. Lekkerkerker, *Nature* **2000**, *406*, 868.
[10] L.-S. Li, A. P. Alivisatos, *Adv. Mater.* **2003**, *15*, 408.
[11] K. M. Ryan, A. Mastroianni, K. A. Stancil, H. Liu, A. P. Alivisatos, *Nano Lett.* **2006**, *6*, 1479.
[12] S. Gupta, Q. Zhang, T. Emrick, T. P. Russell, *Nano Lett.* **2006**, *6*, 2066.
[13] R. Zana, Y. Talmon, *Nature* **1993**, *362*, 228.
[14] J. Pérez-Juste, I. Pastoriza-Santos, L.-M. Liz-Marzán, P. Mulvaney, *Coord. Chem. Rev.* **2005**, *249*, 1870.
[15] R. Zia, J. A. Schuller, A. Chandran, M. L. Brongersma, *Mater. Today* **2006**, *9*, 20.
[16] B. Nikoobakht, M. A. El-Sayed, *Chem. Mater.* **2003**, *15*, 1957.
[17] J. Pérez-Juste, L. M. Liz-Marzan, S. Carnie, D. Y. C. Chan, P. Mulvaney, *Adv. Funct. Mater.* **2004**, *14*, 571.
[18] C. J. Johnson, E. Dujardin, S. A. Davis, C. J. Murphy, S. Mann, *J. Mater. Chem.* **2002**, *12*, 1765.
[19] H. Nakashima, K. Furukawa, Y. Kashimura, K. Torimitsu, *Langmuir* **2008**, *24*, 5654.

[20] K. Mitamura, T. Imae, N. Saito, O. Takai, *J. Phys. Chem. B* **2007**, *111*, 8891.
[21] C. J. Orendorff, T. M. Alam, D. Y. Sasaki, B. C. Bunker, J. A. Voigt, *ACS Nano* **2009**, *3*, 971.
[22] R. Oda, I. Huc, M. Schmutz, S. J. Canday, F. C. MacKintosh, *Nature* **1999**, *399*, 566.
[23] F. M. Menger, J. S. Keiper, *Angew. Chem.* **2000**, *112*, 1980 – 1996; *Angew. Chem. Int. Ed.* **2000**, *39*, 1906.
[24] Q. Liu, M. Guo, Z. Nie, J. Yuan, J. Tan, S. Yao, *Langmuir* **2008**, *24*, 1595.
[25] M. S. Bakshi, F. Possmayer, N. O. Petersen, *J. Phys. Chem. C* **2008**, *112*, 8259.
[26] M. Grzelczak, J. Pérez-Juste, P. Mulvaney, L. M. Liz-Marzán, *Chem. Soc. Rev.* **2008**, *37*, 1783.
[27] J. Gao, C. M. Bender, C. J. Murphy, *Langmuir* **2003**, *19*, 9065.
[28] M. Dreja, W. Pyckhout-Hintzen, H. Mays, B. Tieke, *Langmuir* **1999**, *15*, 391.
[29] S. Manne, T. E. Schäffer, Q. Huo, P. K. Hansma, D. E. Morse, G. D. Stucky, I. A. Aksay, *Langmuir* **1997**, *13*, 6382.
[30] A. Guerrero-Martínez, G. González-Gaitano, M. H. Viñas, G. Tardajos, *J. Phys. Chem. B* **2006**, *110*, 13819.
[31] W. Cheng, M. J. Campolongo, J. J. Cha, S. J. Tan, C. C. Umbach, D. A. Muller, D. Luo, *Nat. Mater.* **2009**, *8*, 519.
[32] A. Guerrero-Martínez, M. A. Palafox, G. Tardajos, *Chem. Phys. Lett.* **2006**, *432*, 486.

